crystals

MDPI

Article

Comparative Study on the Sand Bioconsolidation through Calcium Carbonate Precipitation by *Sporosarcina pasteurii* and *Bacillus subtilis*

Chun-Mei Hsu [1], Yi-Hsun Huang [2], Vanita Roshan Nimje [3], Wen-Chien Lee [1], How-Ji Chen [2], Yi-Hao Kuo [2], Chung-Ho Huang [4], Chien-Cheng Chen [5] and Chien-Yen Chen [6,7,*]

1 Department of Chemical Engineering, National Chung Cheng University, Chiayi 62102, Taiwan; gupi_girl@livemail.tw (C.-M.H.); chmwcl@ccu.edu.tw (W.-C.L.)
2 Department of Civil Engineering, National Chung-Hsing University, Taichung 40227, Taiwan; x699237014x@gmail.com (Y.-H.H.); hojichen@nchu.edu.tw (H.-J.C.); yhkao31@gmail.com (Y.-H.K.)
3 Department of Biomedical Sciences, National Chung Cheng University, Chiayi 62102, Taiwan; vanita.nimje@gmail.com
4 Department of Civil Engineering, National Taipei University of Technology, Taipei 10655, Taiwan; cdewsx.hch@gmail.com
5 Department of Biotechnology, National Kaohsiung Normal University, Kaohsiung 82444, Taiwan; cheng@nknu.edu.tw
6 Department of Earth and Environmental Sciences, National Chung Cheng University, Chiayi 62102, Taiwan
7 Center for Innovative Research on Aging Society, National Chung Cheng University, Chiayi 62102, Taiwan
* Correspondence: chien-yen.chen@oriel.oxon.org or yen@eq.ccu.edu.tw; Tel.: +886-5-2720411 (ext. 66503)

Received: 11 November 2017; Accepted: 21 April 2018; Published: 27 April 2018

Abstract: To investigate potential implications of microbial activity on sand bioconsolidation and subsurface environments, two ureolytic strains, *Sporosarcina pasteurii* and *Bacillus subtilis* were tested for the production of calcium carbonate ($CaCO_3$). Laboratory experiments with monoculture *S. pasteurii* (column 1) and coculture *S. pasteurii-B. subtilis* (column 2) were conducted to determine urea and calcium chloride reactivity and volumetric carbonate formation. Both columns were able to consolidate sand, whereas, column 1 induced greater $CaCO_3$ precipitation. X-ray diffraction (XRD) and scanning electron microscopy (SEM) showed two columns with different mineralogy with calcite, and vaterite formation. Column 1 showed rhombohedral and trigonal crystals morphology, whereas column 2 developed the prismatic calcite and the spherulite vaterite crystals might be due to the differences of the micro-environment caused by the urease expression of these bacterial species. These results indicate the possibility of using those crystals to cement loose sand whereas, highlighted the importance of combining these techniques to understand the geomicrobiology found in the subsurface environments.

Keywords: MICP; *Sporosarcina pasteurii*; *Bacillus subtilis*; bacterial extracellular secretion; urease

1. Introduction

Calcium carbonate ($CaCO_3$) biogenic precipitation is considered as an important process in nature with respect to its role in early diagenesis of marine sediments, hydrochemical evolution of karst streams, application of Geological and Civil Engineering and environmental treatments [1]. From a geotechnical point of view, the potential of microbial carbonate precipitation (MCP) has been identified as a means of adapting soil properties to suit desired land-uses [2]. The reaction is widely distributed in soil, freshwater, marine and subsurface environments. MCP can occur via a variety of processes whereby microbial activities results in the generation of carbonate in a calcium rich environment.

The urea hydrolysis by the enzyme urease of microorganisms in a calcium-rich environment is the most commonly MCP studied. The CO_3^{2-} and NH_4^+ from the hydrolysis of urea increase of the pH and carbonates concentration, which lead to the precipitation of calcium carbonate.

$$CO(NH_2)_2 + 2H_2O \rightarrow 2NH_4^+ + CO_3^{2-} \quad ()$$

$$Ca^{2+} + CO_3^{2-} \rightarrow CaCO_3 \quad ()$$

Through MCP, microbes play an important role in promoting calcite precipitation. Some mechanisms studied by researchers that can induce $CaCO_3$ deposition are: (1) the depositing particles are captured or adhered to by microbial mat or biofilm; (2) extracellular polymeric substances (EPS) can absorb Ca^{2+} so that carbonate microcrystals form on the surface of the biofilm and result in $CaCO_3$ formation; (3) in the environment with higher content of dissolved inorganic carbon (DIC), EPS degradation will release the Ca^{2+} ions that are chelated inside it, so that the supersaturation degree of Ca^{2+} in the environment will be continuously enhanced, resulting in promoting the precipitation of $CaCO_3$; (4) Some bacteria can induce precipitation of $CaCO_3$ extracellularly through such processes as photosynthesis, ammonification, denitrification, sulfate reduction and anaerobic sulfide oxidation; (5) degradation of urea by urea-decomposing bacteria increases pH and alkalinity of the environment, leading to $CaCO_3$ precipitation [3–9]. Mechanisms 1, 2 and 3 are defined as passive forms of precipitation in the presence of organic matter and mechanisms 4 and 5 involve indirect modifications of chemical conditions [4,6]

Considerable research on MCP has been performed using ureolytic bacteria, which influence the precipitation of $CaCO_3$, by the production of the enzyme urease. Urease catalyzes the hydrolysis of urea to CO_2 and ammonia. The resulting $CaCO_3$ precipitation is governed by (1) calcium concentration; (2) carbonate concentration; (3) pH and (4) the use of nucleation sites [10]. The fact that hydrolysis of urea is a straightforward common microbial process and that a wide variety of microorganisms produce the urease enzyme makes it ideally suited for biotechnological applications. Urease activity is widespread among bacteria and this has been the approach most often applied for MCP for the production of calcite [11,12]. Urease-producing bacteria can be grouped into two categories according to their urease response to ammonium; those whose urease activity is not repressed (*S. pasteurii*, *Helicobacter pyroli*) and those whose urease activity is repressed (*Psuedomonas aeruginosa*, *Klensiella aerogenes*) [13,14]. Because high concentrations of urea are hydrolyzed during biocementation, only those microorganisms whose urease activity is not repressed by ammonium are useful. As well as meeting the needs for biocementation, the organism must also meet the needs for safe environmental application. In order to maintain the microbial ecological system in the environment, it will be suitable to apply and release those strains with non-pathogenic, non-genetically modified and non-transferable elements.

S. pasteurii has been widely used as a model organism for the MCP process because this strain is non-pathogenic with significantly high level of urease activity [15]. Calcium carbonate precipitation, a widespread phenomenon among bacteria, has been investigated due to its wide range of scientific and technological implications. Calcite formation by *B. subtilis* (which is a model laboratory bacterium that can produce calcite precipitates on suitable media supplemented with a calcium source) has also been studied [16]. It is also well known that *B. subtilis* was used to produce the varieties of exopolymeric substances, for example, biosurfactants of surfactin. At present, some studies have been done on the role of *B. subtilis* in calcite precipitation. However, there are no adequate studies on the role of calcite precipitation by *B. subtilis* in coculture environments for sand bioconsolidation. We selected *B. subtilis* to study the influence of growth and metabolism of *S. pasteurii* for biocementation processes. In order to clarify the contribution and influence of *B. subtilis*, the monoculture *S. pasteurii* and the coculture *S. pasteurii-B. subtilis* were studied in two different experimental systems. A main part of this research focuses on studying coculture environment for sand bioconsolidation through carbonate precipitation and geomicrobiology in the subsurface environment.

2. Results and Discussion

The effect of two types of microbial systems were evaluated to study the distribution of their activity and calcium carbonate precipitation in sand column through a number of steps elaborated in Table 1.

Table 1. Overview of the column injections for determining microbial carbonate precipitation under monoculture experiment and coculture experiment.

Phase		Description	Duration (h)	Effluent Flow Rate (L/h)	Details
Rinse		Water flush	24	0.2	Tap water
Immobilization of bacteria by two-phase injection	Bacterial injection	1. *S. pasteurii*	24	0.2	OD_{600}: 4.1; Act: 2.13 mS/cm/min
		2. *S. pasteurii* + *B. subtilis*	24	0.2	OD_{600}: 3.2; Act: 1.67 mS/cm/min
	$CaCl_2$ injection	1. *S. pasteurii*	24	0.2	0.05 M $CaCl_2$
		2. *S. pasteurii* + *B. subtilis*	24	0.2	0.05 M $CaCl_2$
Cementation		Reaction fluid injection	24	No flow for 24 h- after 24 h, with 0.2 L/h flow rate, samples were collected	1.1 M Urea and $CaCl_2$
Rinse		Water flush	24	0.2	Tap water

1 and 2 are the column number with specific bacteria. Optical density (OD) and the enzyme activity of the bacterial suspension were measured immediately before injection. For column 2, *S. pasteurii* and *B. subtilis* cultures were taken as 50 *v*/*v* %. Column 3 is not mentioned in the table. Column 3 is the control experiment consisted of uninoculated culture medium along with experimental samples.

Initially, immobilization of bacteria in the column was achieved by a two-phase injection. In order to fill the column volume, bacteria were injected. When bacteria were visualized in the outlet as seen by turbidity, 300 mL of 50 mM calcium chloride solution was injected into the column to immobilize the bacteria in a moving reaction front in the column. To start the cementation, 1.1 M equimolar urea and calcium chloride was injected. Samples were collected at regular intervals to measure OD, pH, urease activity, calcium ammonium concentration measurement [2].

2.1. Optical Density and Urease Activity

Column 1 and column 2 with monoculture and coculture bacteria were studied to elucidate the distribution of urease activity and optical density over the column length. While flushing 300 mL of bacterial suspension, immediately followed by 300 mL fixation fluid of 50 mM $CaCl_2$ solution, measurement of both optical density and urease activity in the effluent of the sand column showed that a large proportion of the injected bacteria was retained in the column (Figure 1a). Further, after injecting the cementation solution, no noticeable activity or bacteria were observed in the effluent (Figure 1b). The effluent measurements showed that bacteria in the monoculture experiment resulted in more wash-out of cells and activity corresponding to that of coculture. This retainment of more urease activity and optical density in coculture may be attributed to the synergistic relationship between *S. pasteurii* and *B. subtilis*, where, in the environment with nutrient limiting conditions or microbes living in deep subsurface, majority of the populations can thrive without any input from the earth's surface. This might be due to the symbiotic association for their survival where organic compounds or metabolites produced by one bacterial species may be utilized by the other to adapt to the harsh environment.

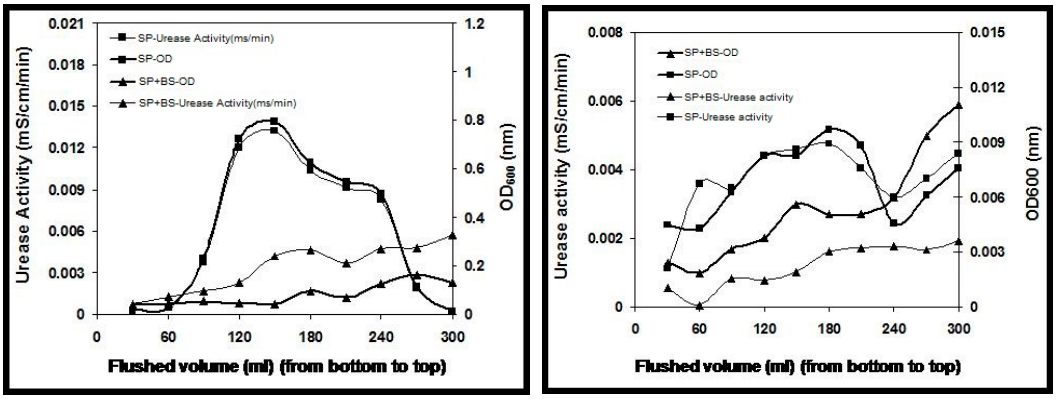

(**a**) (**b**)

Figure 1. (**a**): Effluent measurements for two columns, i.e., monoculture *S. pasteurii* and coculture *S. pasteurii* and *B. subtilis* after flushing 0.05 M $CaCl_2$; (**b**): Effluent measurements for two columns, i.e., monoculture *S. pasteurii* and coculture *S. pasteurii* and *B. subtilis* after flushing cementation solution of 1.1 M Urea and $CaCl_2$.

2.2. Solution Chemistry

The experiments conducted with monoculture and coculture ureolytic bacterial species were monitored for the measurements of pH and NH_4^+ after the column flush. Monoculture *S. pasteurii* and coculture *S. pasteurii-B. subtilis* show almost similar trend in pH over time. During the first batch flush of cementation fluid, the higher pH for column 1 (around 8.6 $\pm$ 1) and only a small pH increase (around 8.3 $\pm$ 1) in coculture experiments for column 2 were observed. Results obtained for the second and third batch flush also correspond to first batch flush with a slight increase of one-two unit pH, which indicates that *S. pasteurii* alone have a strong ureolytic capability to break down the urea while releasing NH_4^+ ions and increasing the solution pH. Similarly, an increase in solution pH for the coculture experiment also shows the strong urease activity in column 2. The control experiment evidenced no change in pH without any bacterial species.

The change in NH_4^+ concentration over time caused by urea hydrolysis for *S. pasteurii* is shown in Figure 2. These values of urea hydrolysis are calculated from measured ammonium concentrations using the stoichiometric equation by Whiffin et al. [2]. One mole of urea is assumed to hydrolyze into two moles of ammonium, and therefore, the amount of urea hydrolyzed at any given time is assumed to be equal to half the amount of ammonia produced. During the first batch flush of cementation, i.e., after 24 h, the maximum NH_4^+ ions produced by *S. pasteurii* in monoculture experiment was 398 mM which further increased to 1160 mM during the second batch flush after 48 h and 1921 mM during the third batch flush after 72 h respectively (Figure 2a). However, the NH_4^+ concentration increased linearly with flushed volume for the entire three-batch flush. To determine the urea hydrolysis under the influence of *B. subtilis* in column 2, a detailed analysis of NH_4^+ ion production was performed. Figure 2b presents the corresponding NH_4^+ concentration values determined during a period of 24, 48 and 72 h. The NH_4^+ concentration does not increase above 157 mM until 24 h during the first batch flush. During the second batch flush with this experiment, NH_4^+ concentration was found to increase to 953 mM, still lower than column 1, whereas, the third batch flush was shown to convert the urea to almost equimolar proportion with a further increase up to 1929 mM. This conclusively shows that urea hydrolysis is occurring for this system and that mono as well as coculture systems can convert the total urea with almost the same rate at the end of the experiment of around 72 h. The NH_4^+ profiles shown in Figure 2a demonstrate that bacterial growth was at its peak in the center of the column where the highest NH_4^+ concentration was measured. In contrast to this, column 2 where no significant bacterial wash out was observed, showed higher NH_4^+ concentrations at the top of the column and was lowest at the bottom.

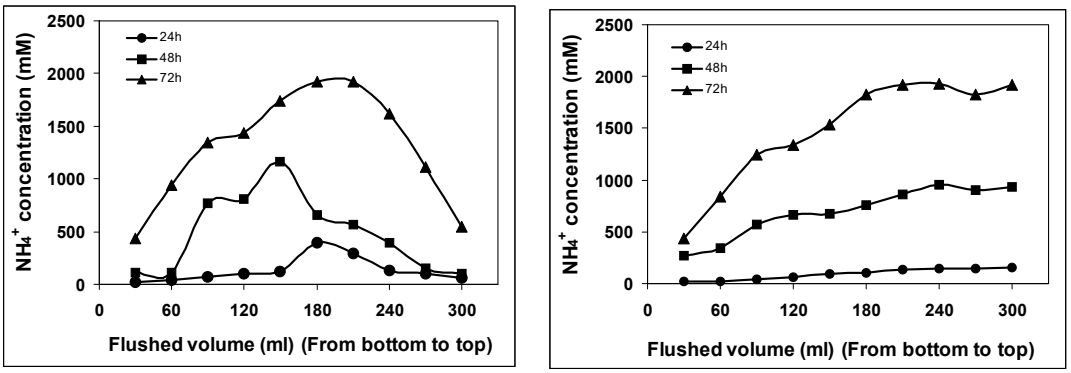

Figure 2. (**a**) Ammonium concentration measurements in the effluent for monoculture *S. pasteurii*, which was flushed out after 24 h, 48 h and 72 h respectively; (**b**) Ammonium concentration measurements in the effluent for coculture of *S. pasteurii* and *B. subtilis*, which was flushed out after 24 h, 48 h and 72 h, respectively.

The trend seen in the calcium precipitation rates mimicked those of NH_4^+ production, i.e., the monoculture of *S. pasteurii* exhibited a faster precipitation rate than coculture over first and second batch flush. Whereas, after a period of 72 h, soluble calcium was detected in the column 1 and column 2 were almost the same which shows that monoculture *S. pasteurii* and coculture *S. pasteurii-B. subtilis* have almost the same ureolytic activity to precipitate $CaCO_3$. The dissolved calcium concentrations over time for monoculture and biculture experiments are shown in Figure 3a,b. Whereas, residual calcium concentrations in the control experiments were higher and remain unreacted corresponding to that of other two systems. This decrease in calcium ion concentration for both the monoculture and biculture experiments could be due to passive precipitation of calcite, with *S. pasteurii* cells acting as nucleation points, or due to sorption of calcium to the cells. Simultaneously, it can be seen from the data that the rate of calcite precipitation was directly proportional to the rate of urea hydrolysis or NH_4^+ production. This results contrasts with that of Stocks-Fischer et al. [17] who stated that calcite precipitation was directly linked to cell growth and indirectly linked to ammonia production. We assume that the results obtained in their study relates to pH where Stocks-Fischer et al. started their experiments at a pH of 8 which is related to the supersaturation degree of the solution for calcite; whereas in the present study, experiments were initiated at a pH of 7.

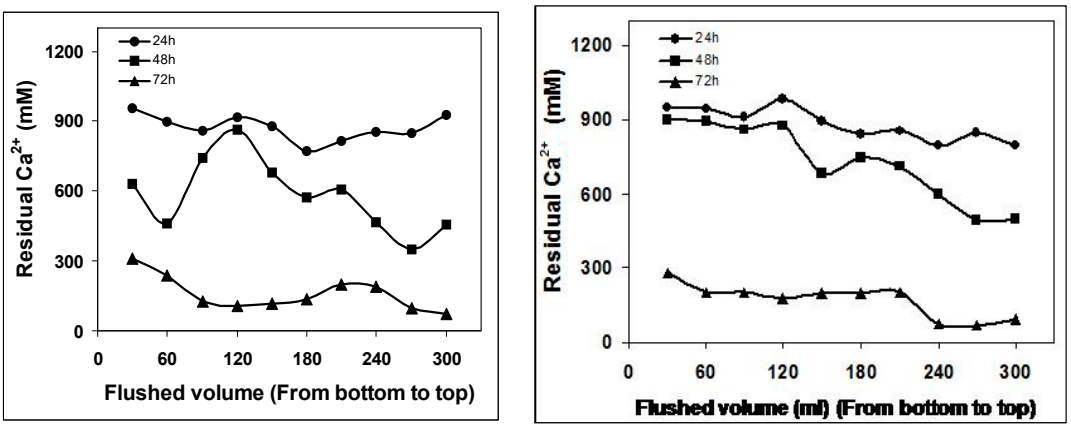

Figure 3. (**a**) Calcium concentration in the effluent for monoculture *S. pasteurii*, which was flushed out after 24 h, 48 h and 72 h respectively; (**b**) Calcium concentration in the effluent for coculture of *S. pasteurii* and *B. subtilis*, which was flushed out after 24 h, 48 h and 72 h, respectively.

2.3. $CaCO_3$ Profile along the Column

After completion of the experiment, all the three columns were flushed for 24 h with tap water and allowed to dry. Samples along the column length were scraped for evaluation of the $CaCO_3$ content. An average $CaCO_3$ content was determined from at least three samples from each column section and results were correlated with the NH_4^+ production of each of the tested samples. For both the columns with monoculture of *S. pasteurii* and coculture *S. pasteurii-B. subtilis* were almost shown to exhibit the same $CaCO_3$ precipitation at the bottom of the column as shown in Figure 4. Whereas the highest strength of $CaCO_3$ formation measured were significantly highest in the middle of the column for monoculture and for biculture highest strength was obtained at the top of the column where maximum $CaCO_3$ precipitation occurred. Hence, by correlating both of these columns for $CaCO_3$ and NH_4^+ concentration, it can be seen that the highest $CaCO_3$ precipitation was measured approximately at the same location where maximum NH_4^+ production was observed with a $CaCO_3$ content of 1.5 kg/m^3 and 1.29 kg/m^3 for monoculture column 1 and coculture column 2, respectively.

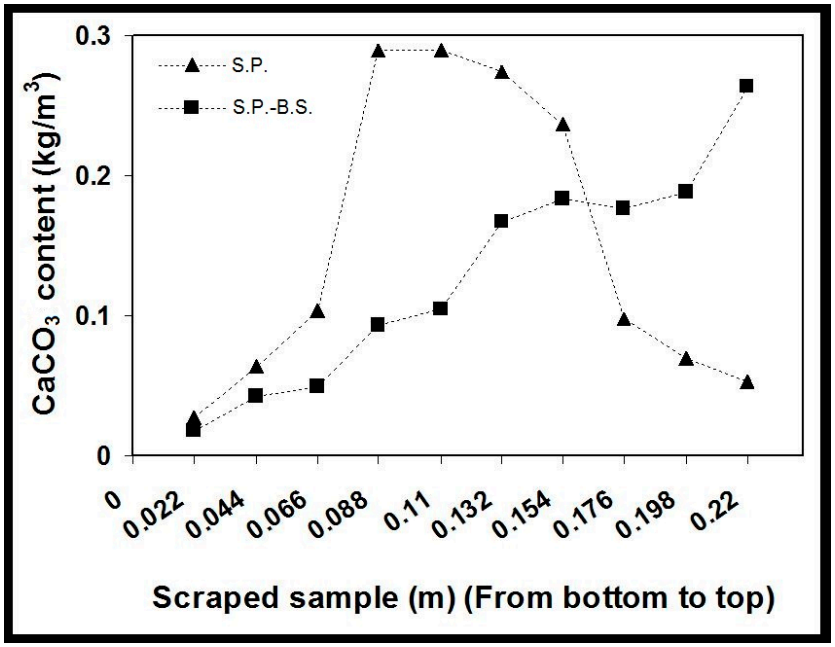

Figure 4. Calcium carbonate profiles along the column length from bottom to top.

2.4. Comparison of XRD Patterns among Monoculture and Biculture Experiments

Figure 5 indicates the results of XRD analyses of $CaCO_3$ precipitation in the sand columns. Sands were carefully removed from $CaCO_3$ precipitates with tweezers before XRD measurements. However, the peaks with strong intensity of 26.62° at the 2θ value that attributed to the Miller indices of (101) of quartz for all the samples were obtained. This is because the Ottawa sand with the size distribution of from 0.1 mm to 1 mm were used. The 2θ values at 20.85°, 26.62° and 40.28° were attributed to the tiny sand quartz particles that remained in $CaCO_3$ precipitates. The XRD peaks located at 2θ values of 29.39°, 36.0°, 39.41°, and 43.10°, which could be assigned to be due to those of calcite, were precipitated by monoculture and coculture bacteria in glass columns. This is coincides with the main characteristic peaks for quartz, and vaterite 26.63 and 26.99, respectively. Those peaks at 2θ of 24.92°, 26.99° and 32.78° might correspond to the vaterite. Aragonite was not detected with XRD and Raman analyses (Supplementary Figures S1 and S2). The Raman active bands at 714 cm^{-1} confirmed the main product of calcite from the MICP process (Supplementary Figure S1). Vaterite is a metastable polymorph of calcium carbonate and is rare in natural environments. It is unstable and rapidly transforms into calcite at room temperature in an aqueous solution [18]. Whereas, bacteria and its secretion (mainly organic

matrix) may facilitate calcium carbonate precipitation. The results showed that both the monoculture *S. pasteurii* and coculture *S. pasteurii-B. subtilis* could induce not only stable calcite crystals but also unstable vaterite crystals. The vaterite crystals have been lasting for more than two years without phase transformation.

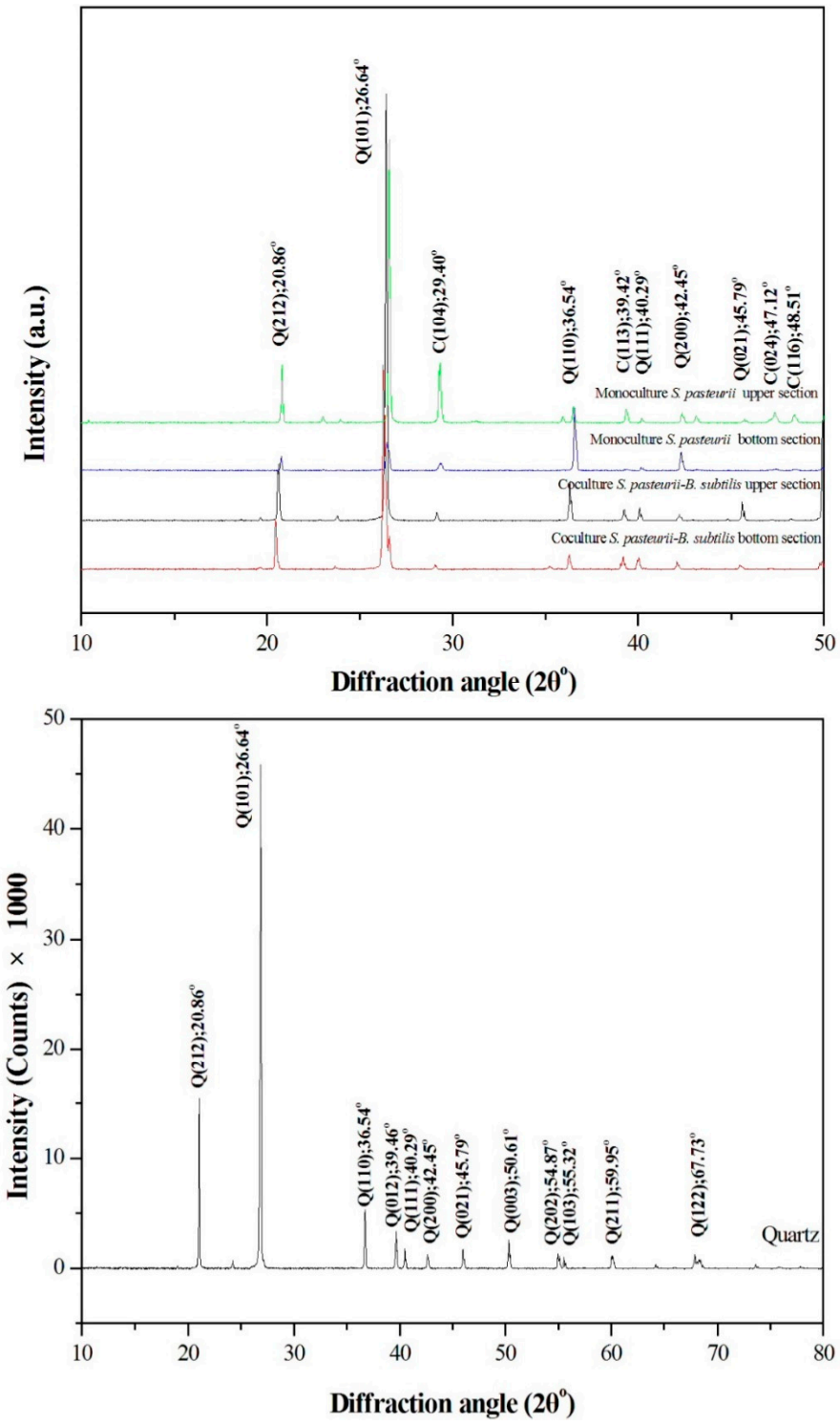

Figure 5. X-ray diffraction of upper and bottom sections for monoculture, coculture. The XRD of quartz only was measured for comparison.

2.5. Comparison of $CaCO_3$ Crystal Morphology Induced by Biological Factors

The $CaCO_3$ crystal morphologies induced by monoculture and biculture experiments are shown in Figure 6. There were obvious differences in the size and morphology of $CaCO_3$ crystals induced in both the experiments as seen in SEM. The column with monoculture *S. pasteurii* exhibited that large amount of $CaCO_3$ particles formed on the top of the column with trigonal prism $CaCO_3$ (about 3 μm) and rod-shaped calcite (25 μm) in Figure 6A, which were accumulated on the sand surface. Furthermore, it was observed that $CaCO_3$ particles were accumulated by compact calcite with irregular flakes of $CaCO_3$ crystals at the bottom of the column (Figure 6A). Those $CaCO_3$ crystals were confirmed by the XRD spectrum in Figure 5. This SEM result evidenced that the action of *S. pasteurii* on specific $CaCO_3$ morphology increased with the increasing depth of the column. However, specific morphology of crystals disappeared at the bottom of the column and irregular compact plate like flakes of $CaCO_3$ appeared probably because the control action of *S. pasteurii* weakened with the gradual bigger and denser crystal size at the top (Figure 6B). Despite the same reaction conditions, coculture bacterial sand columns induced the $CaCO_3$ crystals formation, which were of regular shape; the granular calcite as well as rod-shaped calcite on the top of the column whereas at the bottom of the column compact and lamellar shaped crystals and spherulitic vaterite crystals were induced (Figure 6B). The length/thickness ratio of the rod-shaped crystals in biculture is completely different from monoculture. The main characteristic peaks of calcite can be found from the XRD peaks located at 2θ values of 29.40 in Figure 5. Vaterite was confirmed from the peaks at 2θ of 24.92°, 26.99° and 32.78° (Figure 5). The appearance of vaterite is probably related to the local higher supersaturation of a metastable phase.

The observed carbonate formation under the influence of two bacteria indicates that both the microbes directly participate in crystallization process. In addition, SEM investigation also shows that $CaCO_3$ crystals precipitate in this experimental condition and are approximately of same size of 2–30 μm diameter. However, compared with monoculture, biculture experiments exhibited the three different crystal morphologies, i.e., lamellar, spherulitic and rod. It has been demonstrated that specific biofilm-forming bacteria which could produce exopolysaccharides (EPS) and amino acids play an essential role in the morphology and mineralogy of bacterially induced carbonate precipitation. In a review article, Marvasi et al. [19] described the production of sorptive EPS, poly-γ-glutamate that is anionic, nontoxic and biodegradable viscous polymer produced mainly by wild type *B. subtilis*. In addition, the glutamic acid solution was also shown to induce trigonal prism crystal morphology of $CaCO_3$ precipitate studied by Li et al. [1]. We hypothesize that this is why this crystal morphology was selected in the biculture microbial environment, where the EPS might have been produced by *B. subtilis* which acts as glue to specifically binds Ca^{2+} ions. However, due to its viscous nature, EPS binds more Ca^{2+} ions on the top of the column and it flows slowly down towards the bottom of the column where the $CaCO_3$ precipitation was less. Research conducted by Buczynski and Chafetz [20] showed that EPS plays an important role in the formation of carbonate crystals by providing nucleation sites and by attaching small crystals to each other to increase the size of the bioliths. In accordance with Le Me'tayer-Levrel et al. [21], *B. subtilis* can be applied as biocalcifiers producing carbonates, whereas this activity did not allow the establishment of other bacterial species to function.

Although the present hypothesis that *B. subtilis* EPS/EPS like chemical might release into the environment and influence the $CaCO_3$ formation is from the laboratory experiment, there are wide implications for natural carbonate precipitation, since bacteria are ubiquitous in nature. Thus, this needs to be examined in detail to study the role of *S. pasteurii* and *B. subtilis* monoculture and coculture environment for $CaCO_3$ precipitation and its morphology. Further studies are needed to determine whether the mineralogical biosignatures found in nutrient-rich media can also be found in the subsurface environments.

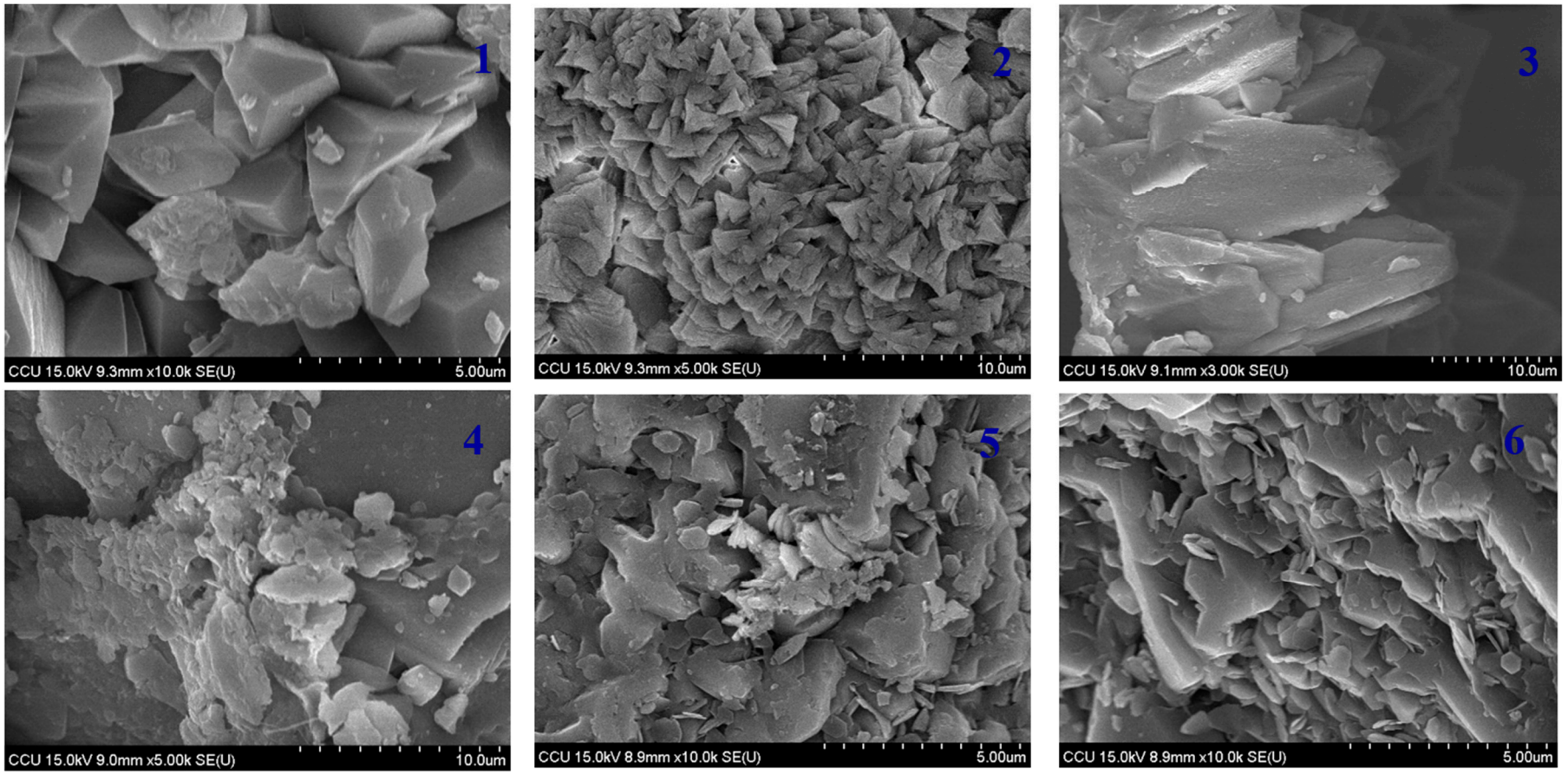

(**A**)

Figure 6. *Cont.*

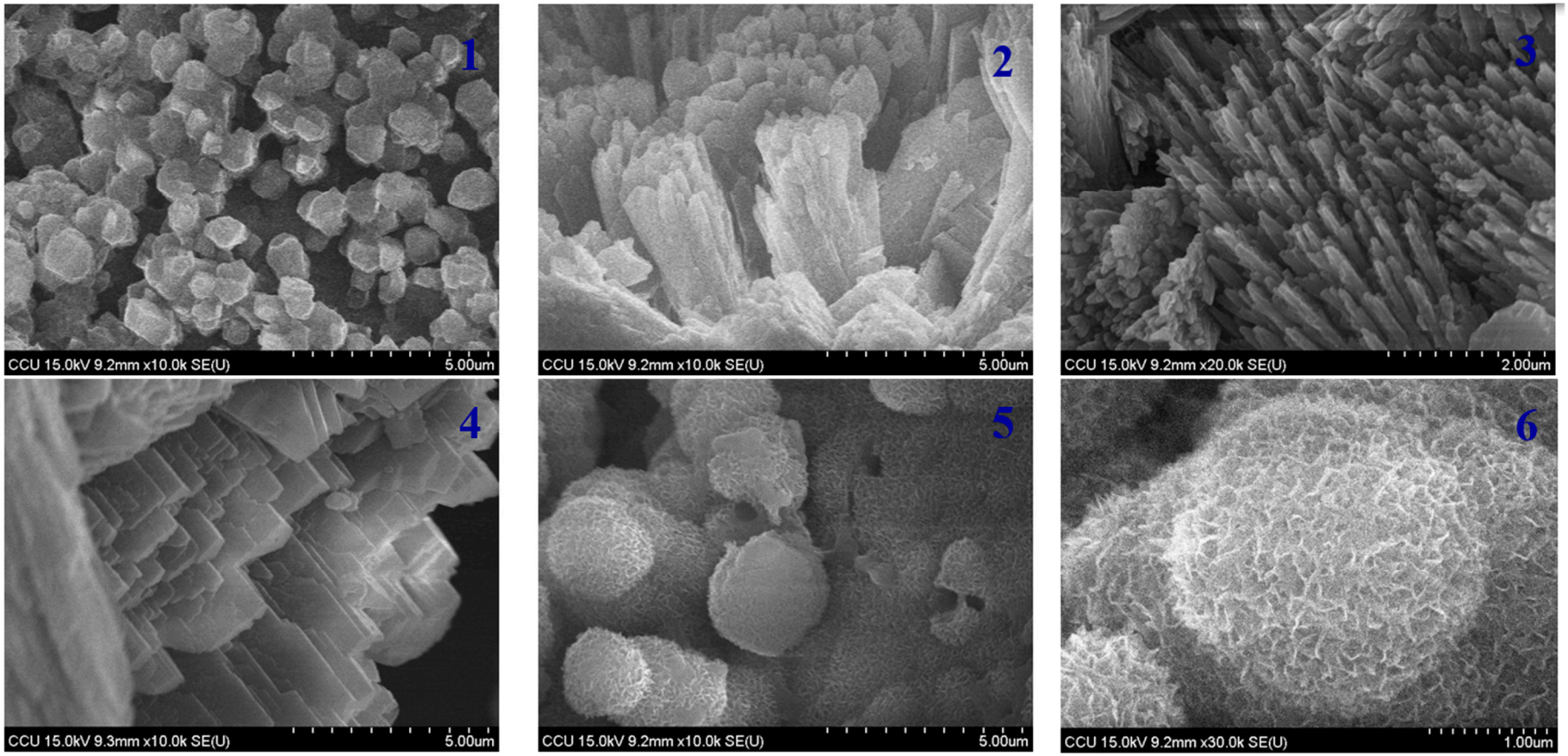

(**B**)

Figure 6. (**A**): SEM imagines of calcium carbonate precipitated by monoculture bacterial experiments. **Top** row (for upper part of column) showed the trigonal prism $CaCO_3$ (1 and 2) and rod-shaped calcite (3). **Down** row (for down part of column) showed the large and compact calcite with the irregular flakes of $CaCO_3$ (4, 5 and 6). (**B**): SEM imagines of calcium carbonate precipitated by coculture bacterial experiments. **Top** raw (for down part of column) showed the granular calcite (1) and rod-shaped calcite (2 and 3). **Down** raw (for upper part of column) showed compact and lamellar calcite (4), and spherulitic vaterite. (5 and 6).

2.6. Engineering Assessment of the Effect of Consolidation

In addition, to verify the effectiveness in consolidation of sand with the two ureolytic stains, *S. pasteurii* and *B. subtilis*, an engineering experiment of mixing standard sand, Portland cement, and bacterial solution into porous cement binder, casting 5 cm cube mortar specimen for testing of compressive strength was carried out.

Figure 7 shows the results of the mortar's compressive strength with different bacterial solutions. The average compressive strength of control specimen without bacteria is 18.2 MPa at 14 days. The mortars incorporated monoculture *S. pasteurii* (SP group) and coculture *S. pasteurii-B subtilis* (SP + BS group) and present the compressive strength of 27.7 MPa and 26.9 MPa, respectively. This indicates that both the monoculture *S. pasteurii* and coculture *S. pasteurii-B subtilis* can greatly enhance the strength of the mortars. It is significant for geotechnical engineering to improve the mechanical property of soil by the invented consolidation method.

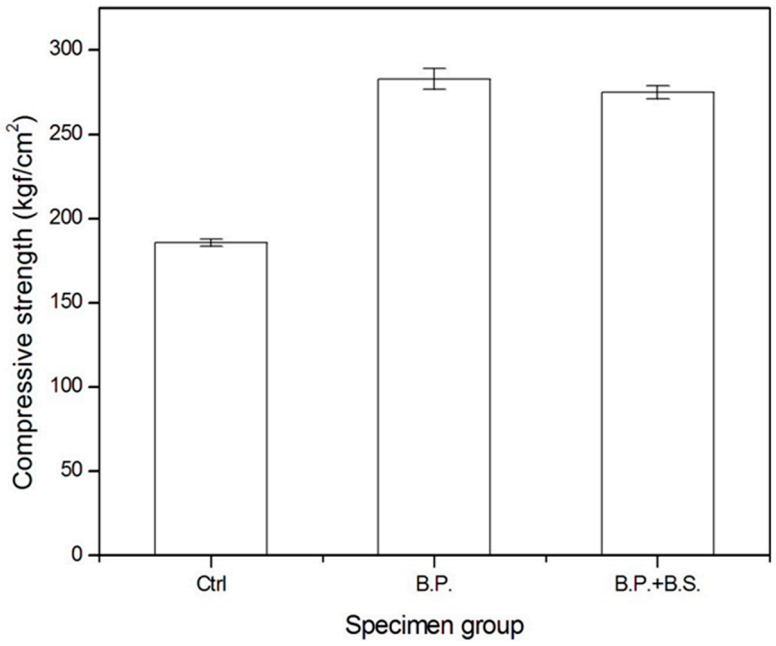

Figure 7. Test results of the compressive strength for the control, SP and SP + BS group specimen at 14 days.

3. Materials and Methods

3.1. Microorganism

The experiments were designed with two aerobically grown bacteria; *S. pasteurii* (DSMZ33) and *B. subtilis* (BBK006). *S. pasteurii* was cultivated under aerobic batch conditions in a medium containing 20 g L^{-1} yeast extract and 10 g L^{-1} NH_4Cl, at a pH of 7. The organism was grown to early stationary phase before harvest. *B. subtilis* was also grown under aerobic batch conditions in M9 medium. The composition of M9 medium was given by Miller as 0.2% glucose in mineral salts (1 g L^{-1} NH_4Cl, 3 g L^{-1} KH_2PO_4, 6 g L^{-1} Na_2HPO_4, 5 g L^{-1} NaCl, 1 mmol L^{-1} $MgSO_4$, and 0.1 mmol L^{-1} $CaCl_2$). Before sterilization, the medium pH was adjusted to 7.0 with 0.5 mol L^{-1} NaOH. The medium was sterilized at 121 °C for 20 min (without glucose for M9 medium, which was filter sterilized (Millipore membrane PVDF, 0.22 μm filter unit; Millipore, Watford, UK) and added afterwards) [22]. Control consisted of uninoculated culture medium along with experimental samples.

3.2. Column Parameters and Sampling

Three cylindrical glass columns (height—0.22 m; internal diameter—0.07 m) were used for this study. The schematic illustration of the setup and sampling positions along the columns were indicated at which the samples were analysed by SEM and XRD as shown in Figure 8. The column was positioned vertically with downward flow direction to avoid any settling of the packing material and generation of preferential flow paths that may occur if the column was positioned horizontally. Each end of the column was fitted with filter material consisting of 1 layers of scouring pad (Scotch Brite) at the outside and approximately 2 cm of filter gravel on the inside, next to the sand. Ottawa sand with the size distribution from 0.1 mm to 1 mm were used. Packing of the sand column was conducted under water to the required density to avoid the inclusion of air pockets. After column packing with sand, the column capacity to hold solution approached to 310 ± 10 mL. A pump was installed at the bottom of the column to regulate the outflow rate of 0.2 L/h. All experiments were performed at ambient temperature of 25 ± 2 °C. During the course of the experiment, samples were taken from the outlet of the column. Immediately after collection, the samples were frozen at −18 °C awaiting analysis. To study, optical density (OD_{600}), pH, urease activity and ammonium concentration samples were centrifuged and the supernatant transferred to a clean tube, which was tested for as required.

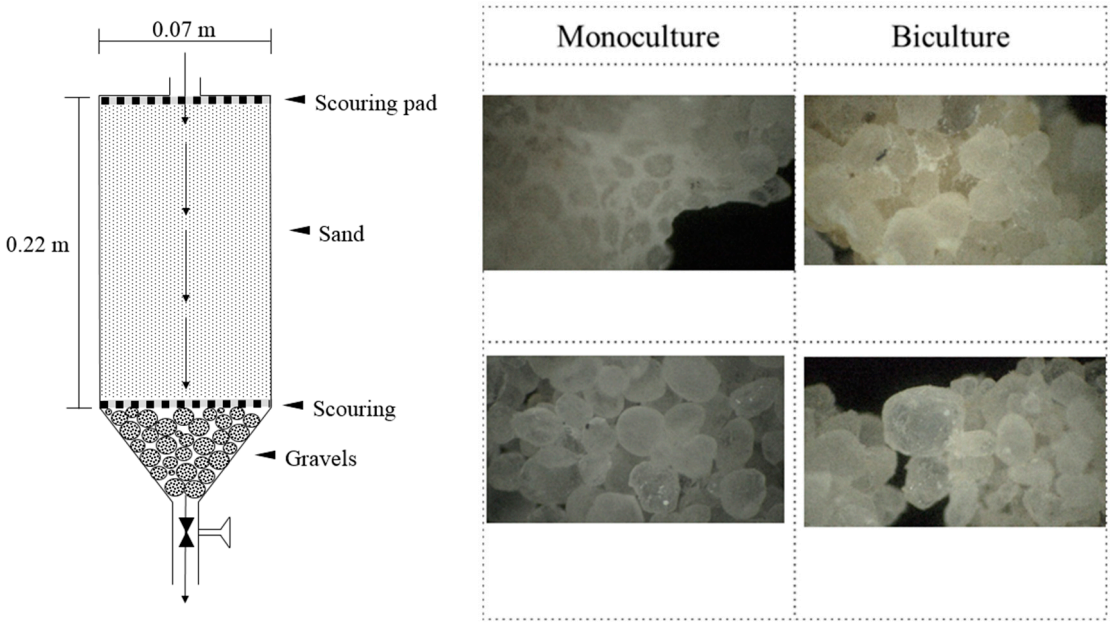

Figure 8. The schematic illustration of the setup and Sampling positions along the columns were indicated at which the samples were analysed by SEM and XRD. The imagines of optical microscopy showed the cemented sands with $CaCO_3$ precipitates for the scraped samples (Magnification = 0.28 × 20 = 5.6).

3.3. Monitoring Methods

Urease activity and NH_4^+ concentration measurements are based upon the work by Whiffin et al. [2].

3.4. Optical Density (OD_{600})

OD was determined using a spectrophotometer and recorded at 600 nm.

3.5. Urease Activity

In the absence of calcium ions, urease activity was determined by a conductivity method. This method was not suitable for determining urease activity in the presence of calcium ions (due to precipitation of calcium carbonate particles and the dampening effect of the counter ion on the solution

conductivity), thus in these cases urease activity was determined from the ammonium production rate. Both methods for determining urease activity were independently calibrated and correlated with each other.

3.6. Ammonium Concentration

Ammonium concentration was determined by a modified Nessler method of Greenburg et al. [23]. The sample was diluted with deionized water to be in the range of 0–0.5 mM. The 2 mL of sample was added to a cuvette and mixed with 100 µL of Nessler reagent (Merck, Kenilworth, NJ, USA), and allowed to react for exactly 1 min. The sample was then read in a spectrophotometer at 425 nm. Absorbance readings were calibrated with several NH_4Cl standards measured under the same conditions.

3.7. Calcium Concentration

Calcium concentration was determined by colorimetric method of Peaslee [24].

3.8. Calcium Carbonate Content

Calcium carbonate content was determined by Loeppert [25]. After drying, the 10 samples were scraped from the top (inlet) to bottom (outlet) of the column. At each sampling point, 3 samples were scraped and averages of them were calculated.

3.9. Flushed Volume

The overall column flow rate was calculated from the total flushed volume (liquid in container plus effluent and port samples) versus time.

3.10. Analysis of Crystal Properties

After drying, the samples were prepared for SEM, XRD and Raman to analyze the crystal properties and minerology. SEM measurements were carried out on a FE-SEM TOPCON field-emission scanning electron microscope (FE-SEM, TOPCON ABT-150S, Singapore). The acceleration voltage of 15 K was used for imaging. Powder X-ray diffraction (XRD) patterns were recorded on a Shimadzu X-ray diffractometer (LabX XRD-6000, Shimadzu, Tokyo, Japan) equipped with Ni-filtered CuKα (λ = 0.1541 nm, 4 kVA, 30 mA) radiation and a graphite crystal monochromator. Raman analysis were performed using inVia reflex Raman Microscopy (Renishaw Plc, Gloucestershire, UK) with the exciting source of He-Cd laser operating at 442 nm with a power of about 80 mW. The measurements were performed for all the three columns and samples for analysis were scraped from the top (inlet) and bottom (outlet) of the column as shown in Figure 8. The scraped samples with sands with $CaCO_3$ precipitates were directly observed using optical microscopy (MEIJI MS-40DR SAM1-P, Saitama, Japan) as shown in Figure 8. The precipitated carbonates were carefully separated from sands with tweezers prior to the XRD and SEM measurements.

3.11. Strength Test of Sand Consolidation

The sample for the strength test of sand consolidation was prepared with mixing standard sand, Portland cement, and bacterial solution into porous mortar. The bacterial solution is SP and SB + BS solution with the OD value of 1.23 and 1.28 respectively. Table 1 gives the mix proportion of the mortars. 3cubes in size of 50 $\times$ 50 $\times$ 50 mm^3 were cast for each specimen group and cured for 24 h at T = 25 °C and 95% $\pm$ 3% relative humidity, then demoulded and cured for 6 days at the same condition as initial. After 7 days, MICP treatments were carried out by the procedures as below:

Samples were immersed in urea solution of 1.1 M for 24 h.

(1) Removing all samples and drying naturally for 24 h.
(2) SB samples were immersed in SP bacterial solution for 24 h, the same procedure as SP + BS.

(3) Removed all samples and dried naturally for 24 h.
(4) All samples were immersed in the mixing solution of 1.1 M urea and 1.1 M calcium acetate for 24 h.
(5) Removed all samples and dried naturally for 48 h. The control group samples were the same procedure as MICP treatments except the procedure of immersed bacterial solution.

The compressive strength test was performed according to ASTM C 109 on 50 mm × 50 mm × 50 mm motar cube at age of 14 days. For each specimen group the compressive strength was the average of three specimens.

4. Conclusions

Microbiological activities that occur in bioconsolidation and subsurface environments are largely unknown. This study documented the impact of carbonate precipitation, mineral/crystal alteration and environmental implication on bioconsolidation of loose sand and subsurface environments. Comparative studies were conducted on the $CaCO_3$ precipitation induced by microbes and other biological factors. The results showed that the precipitation rate of Ca^{2+} in the presence of *S. pasteurii* was faster than that in the presence of *S. pasteurii-B. subtilis,* respectively, but at the end of the experiment, both studies were shown to induce the same precipitation rate. The mineralogical examination and experiments documented the importance of *S. pasteurii* and *B. subtilis* in promoting the formation of calcium carbonate minerals. Our research has extended the understanding of the composition of bacterially precipitated carbonate crystals and evaluated both monoculture and biculture bacteria as a sand bioconsolidant.

Supplementary Materials: The following are available online at http://www.mdpi.com/2073-4352/8/5/189/s1.

Author Contributions: C.-M.H., V.R.N. and C.-C.C. conceived and designed the experiments; C.-M.H., V.R.N. and Y.-H.H. performed the experiments; C.-M.H. and V.R.N., analyzed the data; W.-C.L., Y.-H.K. and C.-H.H. contributed reagents/materials/analysis tools; H.-J.C., C.-Y.C., C.-M.H. and V.R.N. wrote the paper.

Funding: This research was funded by Ministry of Science and Technology Taiwan, grant number [MOST 106-2116-M-194-014].

Acknowledgments: The authors are very grateful to the science council of Taiwan for sponsoring this research.

Conflicts of Interest: The authors declare no conflict of interest.

Abbreviations

$CaCl_2$	Calcium chloride
$CaCO_3$	Calcium carbonate
NH_4^+	ammonium ion
NH_4Cl	Ammonium chloride
Ca^{2+}	calcium ion
XRD	X-ray diffraction

References

1. Li, W.; Liu, L.; Chen, W.; Yua, L.; Li, W.; Yu, H. Calcium carbonate precipitation and crystal morphology induced by microbial carbonic anhydrase and other biological factors. *Proc. Biochem.* **2010**, *45*, 1017–1021. [CrossRef]
2. Whiffin, V.S.; van Paassen, L.A.; Harkes, M.P. Microbial Carbonate Precipitation as a Soil Improvement Technique. *Geomicrobiol. J.* **2007**, *24*, 1–7. [CrossRef]
3. Arp, G.; Hofmann, J.; Reitner, J. Microbial fabric formation in spring mounds ('microbialites') of alkaline salt lakes in the Badain Jaran Sand Sea. *Palaios* **1998**, *13*, 581–592. [CrossRef]
4. Phillips, A.J.; Gerlach, R.; Lauchnor, E.; Mitchell, A.C.; Cunningham, A.B.; Spangler, L. Engineered applications of ureolytic biomineralization: A review. *Biofouling* **2013**, *29*, 715–733. [CrossRef] [PubMed]

5. Perry, C.T. Biofilm-related calcification, sediment trapping and constructive micrite envelopes: A criterion for the recognition of ancient grass-bed environments. *Sedimentology* **1999**, *46*, 33–45. [CrossRef]
6. Benzerara, K.; Miot, J.; Morin, G.; Ona-Nguema, G.; Skouri-Panet, F.; Ferard, C. Significance, mechanisms and environmental implications of microbial biomineralization. *CR Geosci.* **2011**, *343*, 160–167. [CrossRef]
7. Wen, Z.F.; Zhong, J.H.; Li, Y.; Guo, Z.Q.; Gao, J.B.; Xu, X.L. Current study on genesis and formation conditions of stromatolites. *Geol. J. China Univ.* **2004**, *10*, 418–428.
8. Braissant, O.; Decho, A.W.; Przekop, K.M.; Gallagher, K.L.; Glunk, C.; Dupraz, C.; Visscher, P.T. Characteristics and turnover of exopolymeric substances in a hypersaline microbial mat. *FEMS Microbiol. Ecol.* **2009**, *67*, 293–307. [CrossRef] [PubMed]
9. Chen, L.; Shen, Y.H.; Xie, A.J.; Huang, B.; Jia, R.; Guo, R.Y.; Tang, W.Z. Bacteria-mediated synthesis of metal carbonate minerals with unusual morphologies and structures. *Cry. Growth Des.* **2009**, *9*, 743–754. [CrossRef]
10. Hammes, F.; Verstraete, W. Key roles of pH and calcium metabolism in microbial carbonate precipitation. *Rev. Environ. Sci. Technol.* **2002**, *1*, 3–7. [CrossRef]
11. Mobley, H.L.; Hausinger, R.P. Microbial ureases: Significance, regulation, and molecular characterization. *Microbiol. Rev.* **1989**, *53*, 85–108. [PubMed]
12. Fujita, Y.; Ferris, F.G.; Lawson, R.D.; Colwell, F.S.; Smith, R.W. Calcium carbonate precipitation by ureolytic subsurface bacteria. *Geomicrobiol. J.* **2000**, *17*, 305–318. [CrossRef]
13. Friedrich, B.; Magasanik, B. Urease of Klebsiella aerogenes: Control of its synthesis by glutamine synthetase. *J. Bacteriol.* **1977**, *131*, 446–452. [PubMed]
14. Kaltwasser, H.; Krämer, J.; Conger, W.R. Control of urease formation in certain aerobic bacteria. *Arch. Microbiol.* **1972**, *81*, 178–196. [CrossRef]
15. Bachmeier, K.L.; Williams, A.E.; Warmington, J.R.; Bang, S.S. Urease activity in microbiologically-induced calcite precipitation. *J. Biotechnol.* **2002**, *93*, 171–181. [CrossRef]
16. Tiano, P.; Biagiotti, L.; Mastromei, G. Bacterial bio-mediated calcite precipitation for monumental stones conservation: Methods of evaluation. *J. Microbiol. Methods* **1999**, *36*, 139–145. [CrossRef]
17. Stocks-Fischer, S.; Galinat, J.K.; Bang, S.S. Microbiological precipitation of $CaCO_3$. *Soil Biol. Biochem.* **1999**, *31*, 1563–1571. [CrossRef]
18. Spanos, N.; Koutsoukos, P.G. The transformation of vaterite to calcite: Effect of the conditions of the solutions in contact with the mineral phase. *J. Crys. Growth* **1998**, *191*, 783–790. [CrossRef]
19. Marvasi, M.; Visscher, P.T.; Martinez, L.C. Exopolymeric substances (EPS) from *Bacillus subtilis*: Polymers and genes encoding their synthesis. *FEMS Microbiol. Lett.* **2010**, *313*, 1–9. [CrossRef] [PubMed]
20. Buczynski, C.; Chafetz, H.S. Habit of bacterially induced precipitates of calcium carbonate and the influence of medium viscosity on mineralogy. *J. Sed. Res.* **1991**, *61*, 226–233. [CrossRef]
21. Le Metayer-Levrel, G.; Castanier, S.; Orial, G.; Loubiere, J.F.; Perthuisot, J.P. Applications of bacterial carbonatogenesis to the protection and regeneration of limestones in buildings and historic patrimony. *Sediment. Geol.* **1999**, *126*, 25–34. [CrossRef]
22. Miller, H. *Experiments in Molecular Genetics*; CSHL Press: Plainview, NY, USA, 1972.
23. Greenburg, A.E.; Clesceri, L.S.; Eaton, A.D. *Standard Methods for the Examination of Water and Wastewater*, 18th ed.; American Public Health Association: Washington, DC, USA, 1992.
24. Peaslee, D.E. Colorimetric determination of calcium in soil extracts. *Soil Sci.* **1964**, *97*, 248–251. [CrossRef]
25. Loeppert, R.H. *Methods of Soil Analysis—Part 3. Chemical Methods—SSSA Book Series No. 5*; SSSA: Madison, WI, USA, 1996.